Thermoelectric power of ternary semiconductor Se10Sb10Te80 thin films

V. Damodara Das, K. S. Raju, and S. Aruna

Articles you may be interested in

Comparison of crystal growth and thermoelectric properties of n-type Bi-Se-Te and p-type Bi-Sb-Te nanocrystalline thin films: Effects of homogeneous irradiation with an electron beam
J. Appl. Phys. **115**, 214311 (2014); 10.1063/1.4881676

Crystallization behavior in Se90Te10 and Se80Te20 thin films
J. Appl. Phys. **115**, 123506 (2014); 10.1063/1.4869547

Electric current enhanced defect elimination in thermally annealed Bi–Sb–Te and Bi–Se–Te thermoelectric thin films
J. Appl. Phys. **108**, 053711 (2010); 10.1063/1.3477184

The thermoelectric properties and crystallography of BiSbTeSe thin films grown by ion beam sputtering
J. Appl. Phys. **73**, 1252 (1993); 10.1063/1.353266

A twolayer model to explain the thickness dependence of conductivity and thermoelectric power of semiconductor thin films and application of the model to PbTe thin films
J. Appl. Phys. **67**, 3724 (1990); 10.1063/1.345013

Thermoelectric power of ternary semiconductor $Se_{10}Sb_{10}Te_{80}$ thin films

V. Damodara Das[a]
Thin Film Laboratory, Department of Physics, Indian Institute of Technology, Madras, Madras 600 036, India

K. S. Raju and S. Aruna
Department of Crystallography and Bio-Physics, Madras University, Guindy Campus, Madras 600 025, India

Thin films of different thicknesses in the range 400–1600 Å have been vacuum deposited on clean glass substrates held at room temperature by very fast evaporation of the $Se_{10}Sb_{10}Te_{80}$ bulk alloy. The thermoelectric power of these films has been measured as a function of temperature during heating and cooling cycles by the integral method. It is found that the thermoelectric power of these films is slightly different during the heating and the cooling cycles which is ascribed to slight reorientation of microcrystallites as also evidenced by x-ray diffraction. It is further found that the thermoelectric power (at a constant temperature) is a function of film thickness; it varies nearly linearly with reciprocal thickness. From these data, the nature of carrier scattering in the films has been ascertained. From the energy-dispersive x-ray analysis patterns of the films the semiquantitative content of the constituent elements Sb, Se, and Te has been determined. © *1995 American Institute of Physics.*

INTRODUCTION

Ternary and quarternary materials whose major constituent is the chalcogen tellurium are found to be important for use in switching devices, where these materials act as a simple switch because of their voltage-dependent resistance characteristics as detailed below.

These materials are such that when lower voltages are applied across these materials, they exhibit a very high resistance; however, when voltages (or current densities) above a particular critical value are applied, the resistance of these materials falls very sharply to a lower value. Thus, the material effectively acts as a switch of high resistance to the flow of current at low voltages (this constitutes the off position of the switch) and offers very low resistance to the flow of current at voltages above a particular critical value of the voltage (this constitutes the on position).

Similar on/off conditions of this bistable material can also be obtained by other means, for example, by the incidence of light of a particular level or by the application of heat to effect a rise in temperature. In the former case these materials can be used as optical storage memory devices.

The important feature of the on/off states of these bistable materials is that the process is reversible. For example, by the reverse application of the external agency causing the on/off changes, the on state in turn can be reversed to the original off state. Thus, for example, by a decrease in the voltage applied across the material, the material can be brought back from the low-resistance on state to high-resistance off state.

Similarly, the same applies to the light intensity, heat, or temperature pulse. The study of this kind of materials and a search for new switching materials is of importance from the point of view of using these materials for switching devices both in the bulk state and particularly in the thin-film state where the switches can be used in the microelectronic circuits as thin-film switches.

In the literature there is an isolated report[1] about the nonlinear $I-V$ characteristic behavior and possible switching action in the bulk ternary material comprising 80 at. % of tellurium and about 10 at. % each of selenium and antimony. Therefore, it was thought interesting to investigate in the thin-film state the ternary material $Se_{10}Sb_{10}Te_{80}$ to generally characterize this material both electrically and structurally. This article reports the thermoelectric behavior of this material in the thin-film state as a function of film thickness. Interpretation of this behavior has been supported by a structural investigation by x-ray diffractography.

In order to establish the elemental incorporation (Se, Sb, and Te) besides their semiquantitative content in the present thin-film samples, energy-dispersive x-ray analysis (EDAX) work has also been carried out.

EXPERIMENT

The bulk polycrystalline alloy of $Se_{10}Sb_{10}Te_{80}$ was prepared by taking the constituents selenium, antimony, and tellurium in the atomic ratio 10:10:80 in a quartz tube of about 12 mm diameter, and evacuating the tube to a vacuum of about 10^{-5} Torr and then sealing it and heating the sealed quartz tube in a muffle furnace at a slow rate, so that the volatile material selenium completely reacts with the other constituents at a lower temperature slightly above the melting point of selenium at which temperature the sealed tube was kept overnight. This is to ensure that most of the selenium is no longer in the free state.

Then the temperature was raised to the melting points of tellurium and antimony in steps and kept at these temperatures overnight sequentially, so that the complete reaction of the constituents takes place and the ternary alloy is formed. Then the tube was kept at a temperature slightly below the

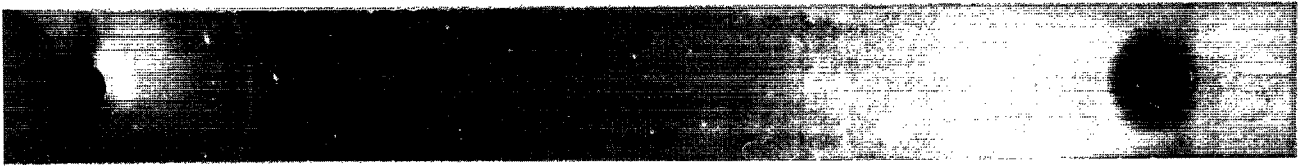[a]Electronic mail: phy10@iitm.ernet.in

FIG. 1. X-ray Debye–Scherrer photograph of the ternary alloy $Se_{10}Sb_{10}Te_{80}$.

melting point of the alloy for 48 h so that the alloy is properly homogenized. Then the tube was cooled to room temperature slowly and then broken open to extract the bulk alloy. The bulk alloy was analyzed by Debye–Scherrer x-ray-powder photography by taking specimens at different positions of the bulk ingot. One of the typical powder photographs is shown in Fig. 1. It was found by Debye–Scherrer x-ray-powder photography that the bulk alloy was homogeneous and the d values of the alloy closely matched those of the binary $Se_{20}Te_{80}$ alloy.[2]

Thin films of $Se_{10}Sb_{10}Te_{80}$ were prepared by vacuum deposition onto cleaned glass substrates held at room temperature in a vacuum of 3×10^{-5} Torr by evaporating small pieces of the bulk alloy from a resistively heated basket-type tantalum boat at a very fast rate in a conventional vacuum deposition system. Thin-film lateral dimensions were 1×7 cm^2. The substrates were kept at a distance of 25 cm vertically above the source.

The films of different thicknesses were prepared during independent pumpdowns, and in each of the depositions the bulk material pieces taken in the boat were completely evaporated at a fast rate so that no residual alloy from a previous deposition was used for any other subsequent deposition. This is to say, each time fresh pieces of the alloy were used for the deposition of different thin films. This procedure is necessary to ensure that there is no change in the composition of thin films as compared to the bulk composition of the alloy due to preferential evaporation of one of the components, the volatile selenium.

The thicknesses of the films were measured by the multiple-beam interferometric technique using a dummy sharp-edged film prepared simultaneously.

The thin films on the glass substrates were mounted for thermoelectric power (TEP) measurements (one at a time) in the experimental setup[3] in the vacuum chamber, and the chamber was evacuated to a vacuum of 3×10^{-5} Torr before making the measurements. The thermoelectric power was measured by the integral method. The films on the glass substrates both immediately after the deposition and after the measurements were also used for x-ray diffractography.

A detailed description of the thermoelectric power measurement setup can be found elsewhere,[3] but, briefly it consisted of a massive copper block in thermal contact with the base plate of the vacuum deposition unit (in which measurements were made) to which one end of the experimental film is clamped. The other end of the experimental film is clamped to a miniheater made of copper so that that end can be heated up to a temperature of about 600 K. During this heating of the hot end of the experimental film the temperature of the cold end (which was clamped to the massive

copper block) was essentially at room temperature and the maximum rise in temperature of the cold end was less than 1 K. Thus, the massive copper block effectively acted as a heat sink.

For EDAX, film-coated glass substrates were cut to the proper size so that they could be mounted onto the aluminum stub and electrical contact was established between the stub and the film using silver paint. The surfaces were examined in the EDAX analyzer no. 711, an accessory to the scanning electron microscope, Philips SEM model 501.

RESULTS AND DISCUSSION

Figure 2 shows the thermal emf developed across the ends of the film as a function of difference in temperature between two ends of the film, for two typical thin films of different thicknesses. For the thermoelectric power measurements, annealed copper wires of the thermocouple quality were used. As the absolute TEP of copper is only 1.7 μV/K compared to very large TEP values of our experimental films, it was neglected in comparison to the TEP of our films.

From the figure we see that the thermal emf increases somewhat linearly at low-temperature differences but in-
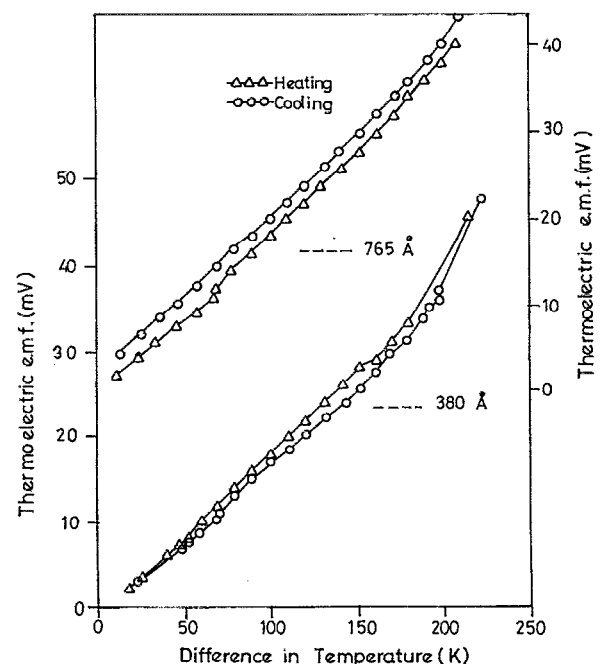

FIG. 2. Thermal emf vs temperature difference plots of two typical thin films.
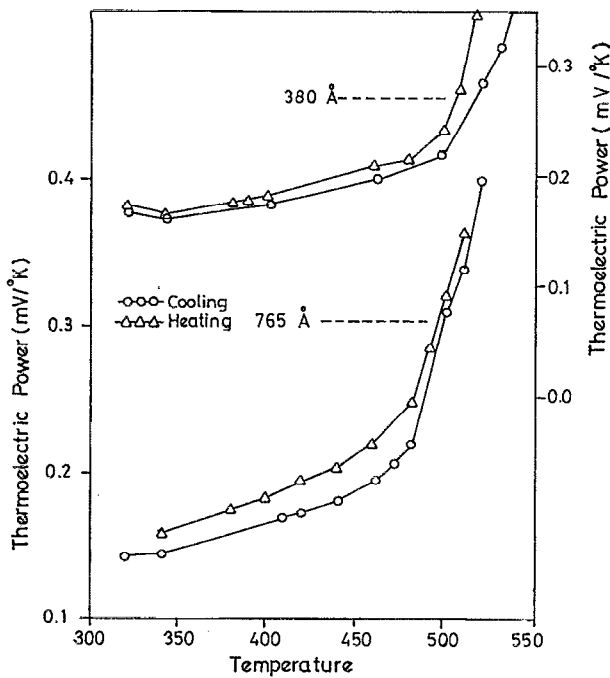
                                    Damodara Das, Raju, and Aruna

FIG. 3. Thermoelectric power vs temperature plots for the above films.

FIG. 4. Thermoelectric power vs reciprocal temperature plots for the above thin films.

creases at a fast rate at higher temperature differences of 200 K or more. We also find that the thermal emf developed during cooling is slightly larger than that during heating at all the temperatures. This can be attributed to the reorientation of microcrystallites of the films upon heating during the first measurement. As pointed out later, a slight reorientation of the microcrystallites is also verified by the change in intensities of the various peaks at one another's expense as seen by x-ray diffractometry before and after heating during thermoelectric measurements.

From the terminals of the voltmeter to which the hot and cold ends of the thin film were connected it was found that the TEP of the films was negative. It can also be noted that the thermal emf developed for a particular difference in temperature while cooling is higher than that developed while heating. This is due to partial evaporation of the material from the films at higher temperatures and also due to some structural rearrangements during heating.

Figure 3 shows the plots of thermoelectric power of two typical films (whose thermal emf versus temperature difference plots are shown in Fig. 2) as a function of temperature both during heating and cooling.

It is found again from the figure that for all temperatures and for all the films the TEP also is higher (at a particular temperature) while cooling than while heating. Another point to be noted from the figures is that at a temperature below about 450–500 K the TEP varies slowly with temperature but above about 475 K it increases at a very fast rate with increase in temperature.

Figure 4 shows the TEP plots of two typical films as a function of reciprocal temperature. It is found that all the plots are curves and only at the highest temperature where there is a steep increase of TEP with temperature can the data points be considered to lie on straight lines but the slopes of
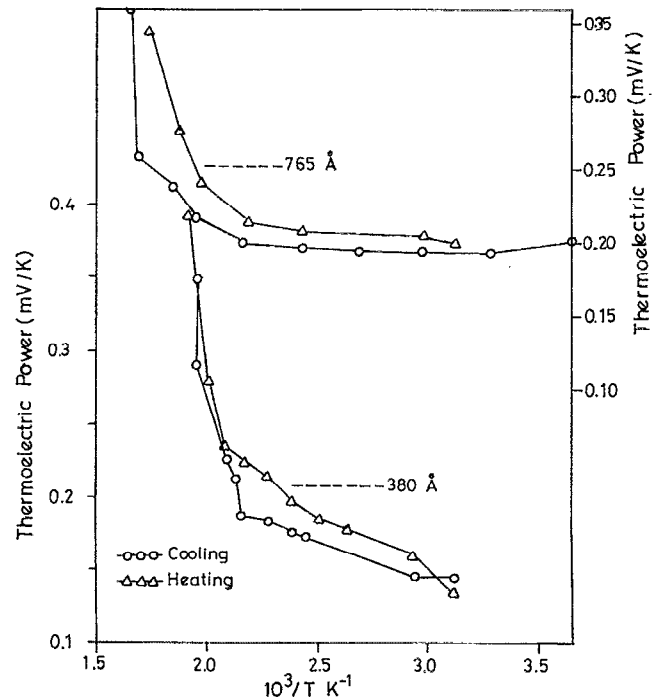
these lines are very large and close to ∞, and the data points at high temperatures are very few and hence no attempt is made to analyze these linear curves further. It can be said that, as expected in the case of semiconductors, the linear variation of TEP as a function of reciprocal temperature $(1/T)$ at high temperatures indicates that the material films are indeed semiconducting.

Figures 5(a) and 5(b) show the plots of TEP as a function of thickness and reciprocal thickness, respectively, at different temperatures. It is seen from the figures that the TEP of the films is a function of thickness, and Fig. 5(b) shows that the TEP is a near-linear function of reciprocal thickness as expected from the classical size effect theories[4–10] at all the four temperatures for which the data have been plotted.

It is well known[4–10] that the thermoelectric power of a thin film is a function of film thickness and varies linearly as the inverse thickness.

The equation for the TEP of thin films as mentioned in the Refs. 9 and 10 is

$$S_F/S_g = 1 - (3/8)(1-p)(l_g/t)[U_g/(1+U_g)],$$

where S_F is the thermoelectric power of the thin film. S_g is defined as the "grain-boundary thermoelectric power" which is the thermoelectric power of a bulk material (film of infinite thickness) of the same microcrystallite size as that of the experimental films. l_g is the mean free path of the charge carriers in the above bulk material having the filmlike microcrystallites mentioned above, and p is the specularity parameter which gives the fraction of the charge carriers scattered specularly from the film surfaces (both internal and external).
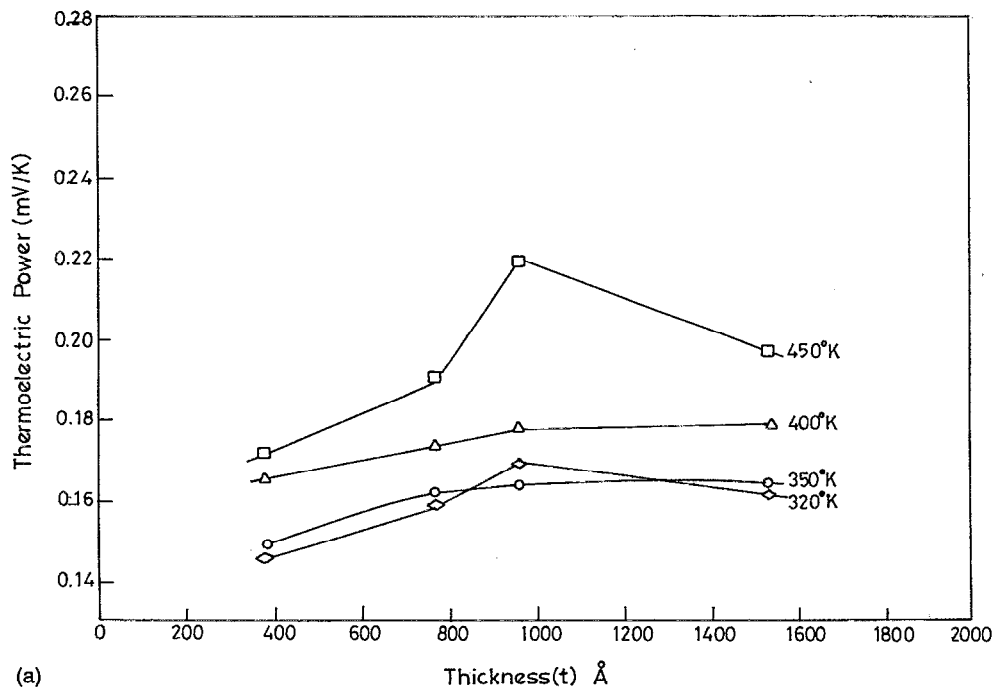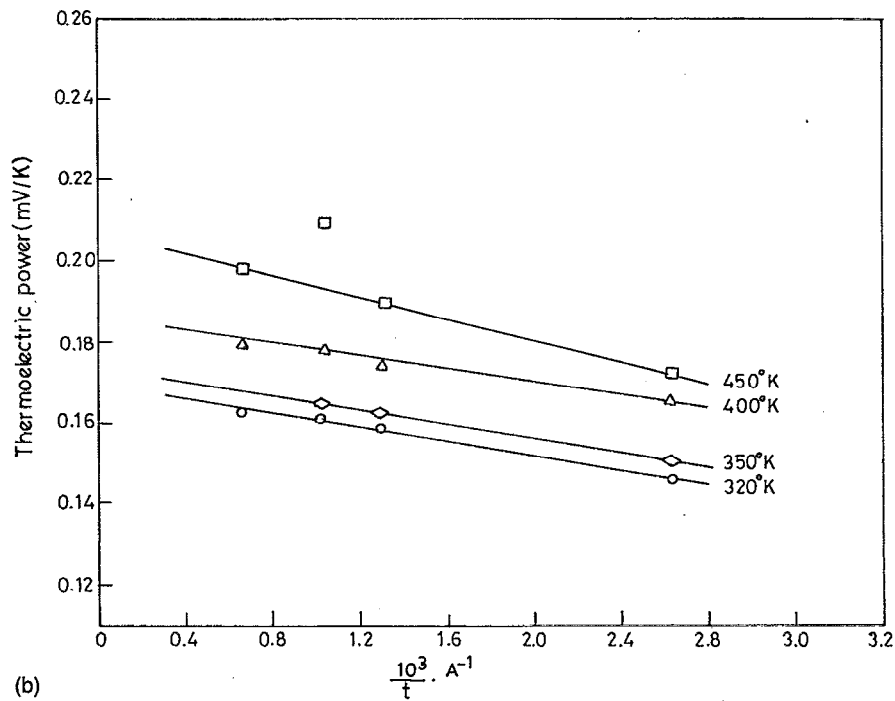
FIG. 5. Thermoelectric power vs film thickness and reciprocal thickness at different temperatures.

U_g is the logarithmic derivative of the above mean free path l_g with the carrier energy E evaluated at the Fermi energy, $(d \ln l_g/d \ln E)_{E=E_F}$.

Assuming that the scattering from the film surfaces is diffuse (i.e., $p=0$) and taking the mean-free-path value of bulk tellurium as the grain-boundary mean free path l_g of the films, the rate of variation of the mean free path with energy of the charge carriers U_g can be evaluated at different temperatures.

It is found that the U_g values are as tabulated in Table I. These values give the power index n in the energy dependence of the mean-free-path equation $l=l_0 E^n$ where we assume the mean free path to be a power function of energy.

Figures 6(a) and 6(b) show the x-ray diffractograms of the as-grown film and of the film after heating during the thermoelectric measurements. It is seen from the diffractograms that one of the peaks marginally increases in intensity at the expense of the other. This indicates that there is some

Damodara Das, Raju, and Aruna

TABLE I. Variation of S_g and U_g with temperature.

Temperature (K)	S_g (μV/K)	U_g
320	170	0.19
350	174	0.17
400	187	0.15
450	270	0.16

reorientation of microcrystallites during heating during thermoelectric measurements. Also, there can be removal of frozen-in defects during heating. Both these reasons explain the difference in the thermal emf developed for the same temperature difference (thus also the difference thermoelectric power values) during the heating cycle and the cooling cycle.

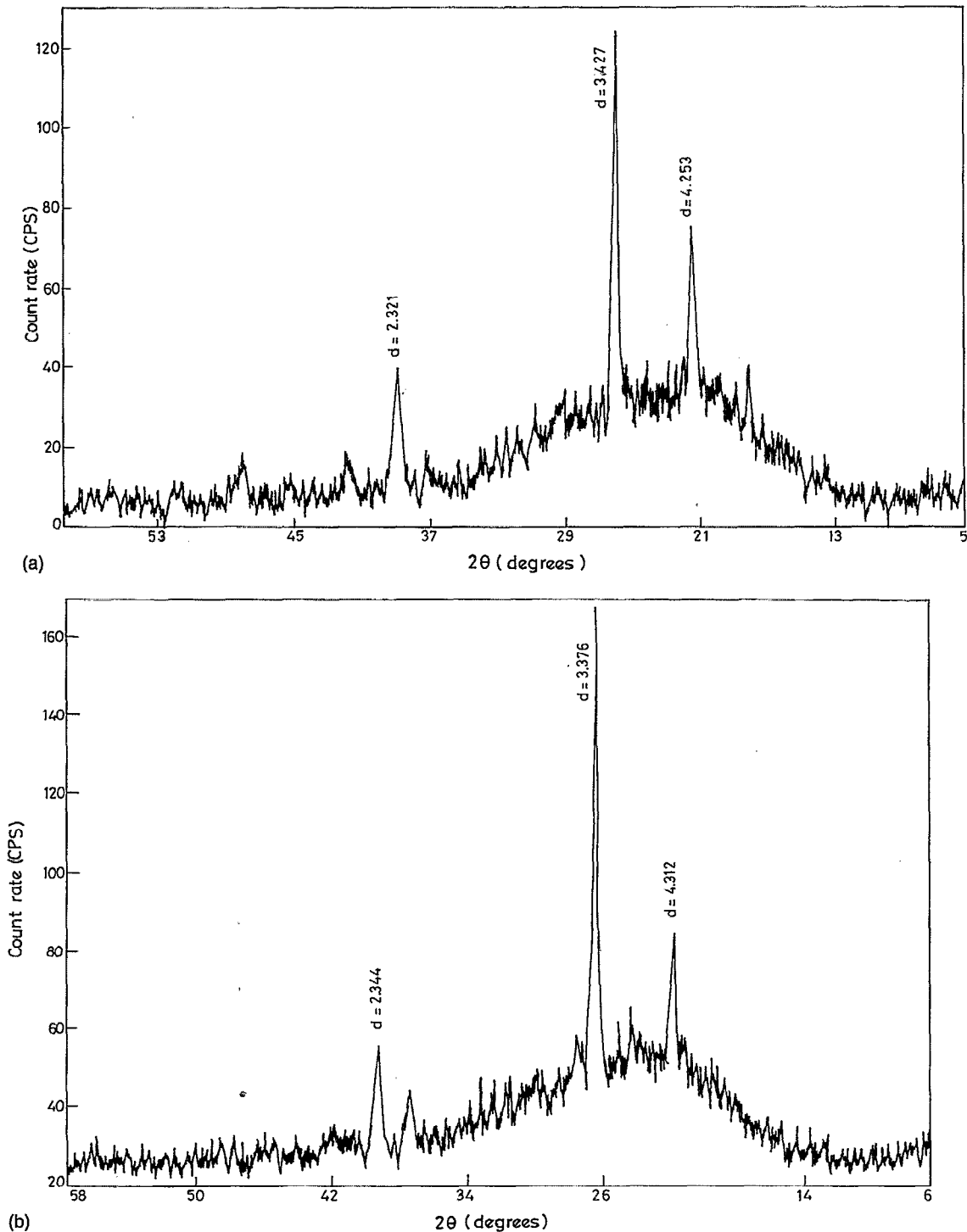Figure 7 shows the EDAX pattern of the thin-film

FIG. 6. X-ray diffractograms of (a) the as-grown film and (b) after heating during thermoelectric measurements.
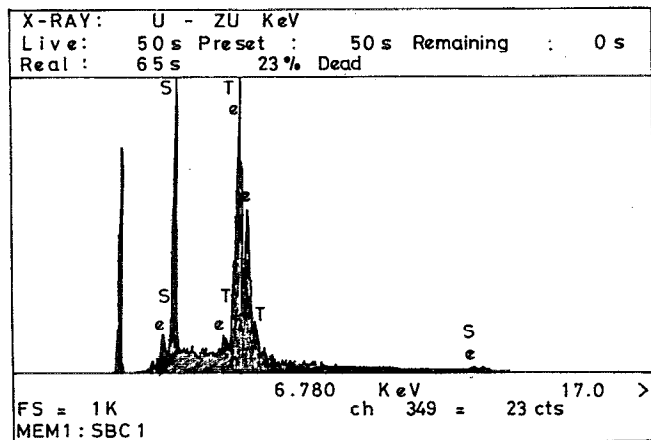
```
X-RAY:    U - ZU  KeV
Live:     50s Preset :    50s Remaining    :   0s
Real :    65s       23% Dead


          S    T
               e



     S         T
     e         e    T


                         S
                         e


                6.780   KeV           17.0   >
                     ch  349  =   23 cts
FS = 1K
MEM1 : SBC 1
```

FIG. 7. EDAX pattern of the thin-film sample.

TABLE II. EDAX peak data.

Element	ZAF	% element	at. %	Normalized composition (w.r. to Te)
Sb	0.979	8.959	8.603	9.8
Se	0.867	14.139	20.935	24.0
Te	1.101	76.902	70.462	80.0
Total		100.000	100.000	

sample and Table II gives the atomic weight percentage composition of the elements in the sample. It is quite clear from the pattern that the presence of Te and Se is evident from the peaks marked, while Sb is not observed. This can be attributed to the fact that L_α peaks for Sb and Te are very close (3.60 and 3.77 keV) and Sb is in a very low concentration as compared to Te and, hence, Sb L_α is evidently superimposed with Te L_α. Thus, an Sb peak cannot be observed; however, the instrument gives the composition of Sb also in the alloy films. The atomic weight percentages given in the table may be on the lower-value side, as during analysis the incident electron beam can cause evaporation of the volatile film components.

The areas (and heights) under the EDAX peaks relating to Te (L_α) and Sb (L_α) as given by the instrument agree with their respective contents in the bulk ternary alloy. However, the content of the volatile Se is as high as 20%–25% in the films of the alloy, which is ascribed to the preferential evaporation of the volatile Se during the evaporation of the bulk alloy.

CONCLUSIONS

The thermoelectric power of the films is negative and it increases moderately slowly at low temperatures and at a very fast rate above about 475 K. It is also found that the TEP is nearly linearly proportional to the reciprocal thickness. Using the S_F versus reciprocal thickness plots, the scattering parameter U_g giving the power index of the energy dependence of the mean free path has been evaluated at different temperatures. Areas (and heights) under the EDAX peaks relating to Te$_{L_\alpha}$ and Se$_{L_\alpha}$ agree well with the respective content in the bulk alloy. However, the content of volatile selenium in thin films is more than doubled.

[1] J. K. Zope, Ind. J. Pure Appl. Phys. **20**, 774 (1982).
[2] V. Damodara Das and P. Jansi Lakshmi, J. Mater. Sci. **23**, 3869 (1988).
[3] V. Damodara Das and J. Chandra Mohanty, J. Appl. Phys. **54**, 977 (1983).
[4] H. Mayer, in *Structure and Properties of Thin Films*, edited by C. A. Neugebauer, J. B. Newkirk, and D. A. Vermilyea (Wiley, New York, 1957), p. 225.
[5] W. F. Leonard and S. F. Lin, J. Appl. Phys. **41**, 1862 (1970).
[6] C. R. Tellier, C. R. Pichard, and A. J. Tosser, Thin Solid Films **42**, L31 (1977).
[7] C. R. Tellier and A. J. Tosser, Thin Solid Films **41**, 161 (1977).
[8] F. Warkusz, Thin Solid Films **52**, L9 (1978).
[9] C. R. Tellier, Thin Solid Films **51**, 311 (1978).
[10] C. R. Tellier, A. J. Tosser, and C. Boutrit, Thin Solid Films **44**, 201 (1977).